Supporting Information:

Convergence of theory and experiment on the role of preorganization, quantum tunneling and enzyme motions into flavoenzyme-catalyzed hydride transfer

Manuel Delgado,[†,#] Stefan Görlich,[‡,#] James E. Longbotham,[‡,I] Nigel S. Scrutton,[‡] Sam Hay,[‡,*] Vicent Moliner,[†, ¥,*] Iñaki Tuñón,[§,*]

[†]Department of Physical and Analytical Chemistry, University Jaume I, 12071, Castelló de la Plana, Spain

[‡]Manchester Institute of Biotechnology and School of Chemistry, The University of Manchester, 131 Princess Street, Manchester, M1 7DN, United Kingdom.

[I]Current address: Department of Cellular and Molecular Pharmacology, University of California San Francisco, San Francisco, CA 94158-2140.

[§]Department of Physical Chemistry, University of València, 46100, Burjassot, Spain.

[¥] Department of Chemistry, University of Bath, Bath BA2 7AY, United Kingdom.

[#]These authors contributed equally.

Correspondig authors

*S.H., e-mail, sam.hay@manchester.ac.uk

*V.M, e-mail, moliner@uji.es

*I.T., e-mail, ignacio.tunon@uv.es

Table S1. Limiting rate constants (k_{lim}), apparent saturation constants (K_S) and KIEs on k_{lim} for the reaction of morphinone reductase with each coenzyme isotopologue

Coenzyme isotopologue	k_{lim} (s^{-1})	K_S (mM)	KIE_{lim}
NADH	55.8 ± 1.1	0.13 ± 0.01	-
(*R*)-[4-^{2}H]-NADH	7.92 ± 0.14	0.09 ± 0.01	7.05 ± 0.26
(*S*)-[4-^{2}H]-NADH	43.6 ± 1.7	0.11 ± 0.01	1.28 ± 0.08
(*R,S*)-[4-$^2H_2$]-NADH	6.68 ± 0.08 (6.43 ± 0.08)	0.09 ± 0.01	8.36 ± 0.26 (8.68 ± 0.28)

Data are taken from the Figure 3. As the (*R,S*)-[4-$^2H_2$]-NADH contained significant ^{1}H contamination at the C4 pro-*S* position (Figure S1), the observed rate constant and resulting KIE was corrected by linear extrapolation (Figure S2).[1] Corrected values are given in (parenthesis) and the correction has no effect on the magnitude of K_S. Note: We are only interested in the value of k_{lim} as this is the intrinsic rate of FMN reduction/hydride transfer from which the KIEs are determined. K_s is given only for completeness.

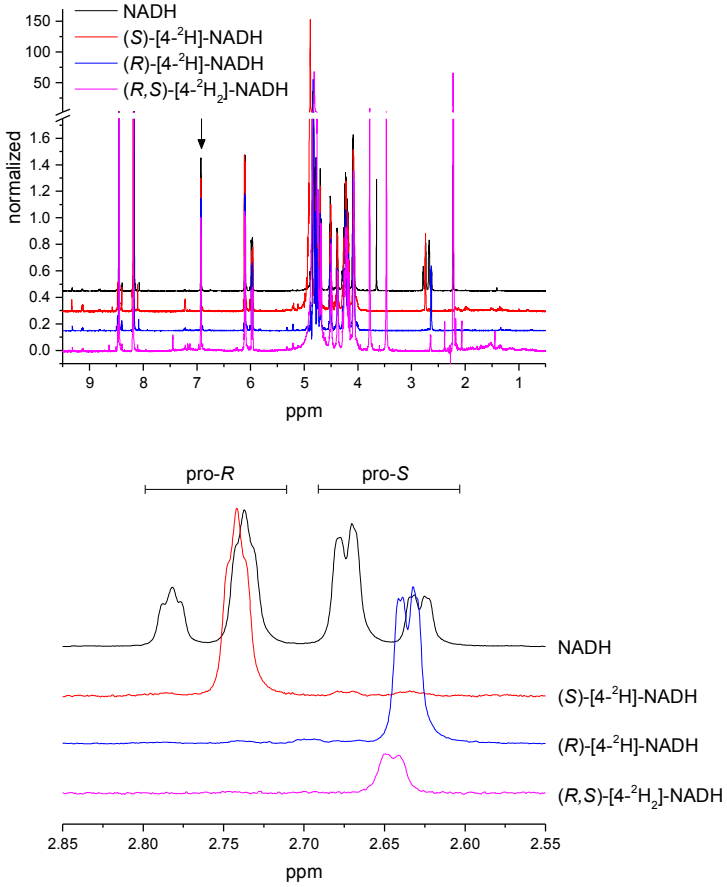

Figure S1. ^{1}H NMR spectra of the NADH isotopologues. Spectra are normalized to the C2 proton marked with an arrow in the top panel and the bottom panel shows an expansion of the spectra around the C4 pro-*R* and pro-*S* protons. Isotopic purities of each isotopologue are given in Table S2. Samples were in 100% D_2O and spectra were recorded on a Bruker UltraShield 400 MHz spectrometer at 298 K.

Table S2. Isotopic purity (fraction ^{1}H) at the C4 position of each coenzyme isotopologue.

Coenzyme isotopologue	pro-*R*	pro-*S*
NADH	0.98	0.98
(*S*)-[4-^{2}H]-NADH	0.99	0.04
(*R*)-[4-^{2}H]-NADH	0.01	0.97
(*R,S*)-[4-$^{2}H_2$]-NADH	0.00	0.21

Data were determined by integration over the regions shown in Figure S2 after the spectra were normalized to the C2 proton (integral = 1.00). Error in these values is taken to be ± 0.01.

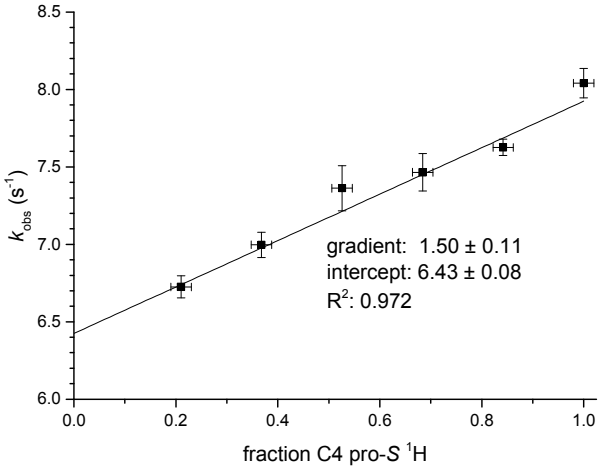

Figure S2. Correction of the observed rate of MR reduction by (*R,S*)-[4-$^{2}H_2$]-NADH for the isotopic impurity at the C4 pro-*S* position (Figure S2, Table S2). The observed rate was measured with mixtures of by (*R*)-[4-$^{2}H_2$]-NADH and (*R,S*)-[4-$^{2}H_2$]-NADH (5 mM total post-mixing concentration) essentially as described previously.[1] The trend is apparently linear, so the corrected (*R,S*)-[4-$^{2}H_2$]-NADH k_{obs} is taken to be the intercept (6.43 ± 0.08 s^{-1}).

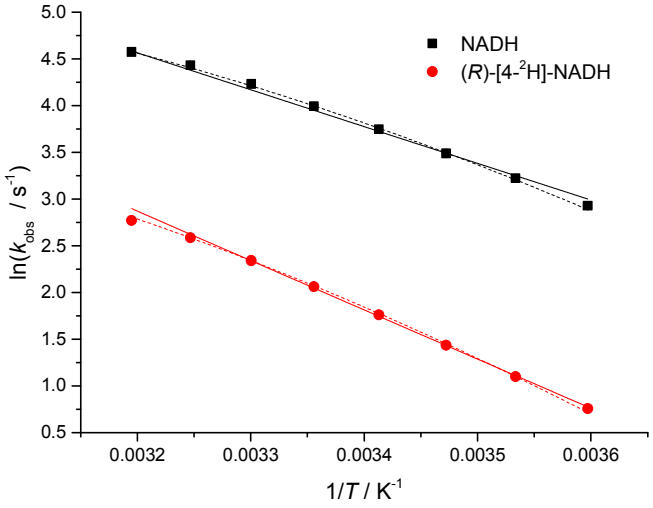

Figure S3. Arrhenius-type plot of the temperature dependence of the observed rate of hydride transfer from NADH and (*R*)-[4-^{2}H]-NADH to the FMN in morphinone reductase. The data are fitted to the non-linear Eyring-based function:

$$\ln k_{obs} = \ln\left(k_B T/h\right) - \left(\Delta H^{\neq}_{T_0} + \Delta C^{\neq}_p (T - T_0)\right)/RT + \left(\Delta S^{\neq}_{T_0} + \Delta C^{\neq}_p \ln(T/T_0)\right)/R$$

where $\Delta C_p^{\ddagger}$ is the difference in heat capacity between the reactant and transition states, $\Delta H_{T0}^{\ddagger}$ and $\Delta S_{T0}^{\ddagger}$ are the activation enthalpy and entropy, respectively at a reference temperature T_0 (298 K in this study) and k_B, h and R are the Boltzmann, Planck and ideal gas constants, respectively.[2,3] Fitting values are given in Table S3 and rate constants are tabulated in Table S4. Measurements were performed with saturating (5 mM post-mixing) concentrations of each coenzyme and ~20 μM (post-mixing) morphinone reductase in 50 mM potassium phosphate, pH 7.0 under anaerobic conditions.

Table S3. Fitting parameters for the fits of the Arrhenius-type data in Figure S3.

parameter	$\Delta C_p^{\ddagger}$ floating	$\Delta C_p^{\ddagger}$ fixed to zero
$\Delta H^{\ddagger H}$, kJ mol^{-1}	31.0 ± 0.3	30.3 ± 0.5
$\Delta H^{\ddagger D}$, kJ mol^{-1}	39.2 ± 0.6	41.4 ± 0.8
$\Delta\Delta H^{\ddagger}$, kJ mol^{-1}	8.3 ± 0.8	11.1 ± 1.3
$\Delta S^{\ddagger H}$, J mol^{-1} K^{-1}	-107.7 ± 0.9	-110.4 ± 1.8
$\Delta S^{\ddagger D}$, J mol^{-1} K^{-1}	-96.0 ± 1.9	-88.9 ± 2.6
$\Delta\Delta S^{\ddagger}$, J mol^{-1} K^{-1}	11.7 ± 2.8	21.5 ± 4.3
$\Delta C_p^{\ddagger H}$, kJ mol^{-1}	-0.48 ± 0.08	-
$\Delta C_p^{\ddagger H}$, kJ mol^{-1}	-0.50 ± 0.11	-
$\Delta\Delta C_p^{\ddagger}$,kJ mol^{-1}	-0.02 ± 0.19	-

Table S4. Tabulated rate constants for the reaction of morphinone reductase with either 5 mM NADH or 5 mM (*R*)-[4-^{2}H]-NADH at 5-40 ^{o}C.

Temperature, ^{o}C	k_{obs}, s^{-1}		KIE_{obs}
	NADH	(*R*)-[4-^{2}H]-NADH	
5	18.72 ± 0.32	2.136 ± 0.041	8.76 ± 0.23
10	25.13 ± 0.17	2.999 ± 0.012	8.38 ± 0.07
15	32.76 ± 0.09	4.207 ± 0.054	7.79 ± 0.10
20	42.44 ± 0.35	5.823 ± 0.069	7.29 ± 0.11
25	54.33 ± 0.74	7.866 ± 0.048	6.91 ± 0.10
30	68.92 ± 0.36	10.40 ± 0.01	6.63 ± 0.04
35	84.20 ± 0.78	13.28 ± 0.07	6.34 ± 0.07
40	97.15 ± 0.20	15.97 ± 0.23	6.08 ± 0.09

Computational details.

The quasi-classical activation free energy at the TS, ΔG_{act}^{QC}, is calculated as:

$$\Delta G_{act}^{QC}(T,\xi)=\left[W^{CM}(T,\xi*)+\Delta W_{vib}(T,\xi*)\right]-\left[W^{CM}(T,\xi_R)+\Delta W_{vib,R}(T)+G_{R,T,F}^{CM}\right] \quad (1)$$

where $\Delta W_{vib}(T,\xi*)\Delta W_{vib}(T,z^*)$ corrects $W^{CM}(T,\xi*)W^{CM}(T,z^*)$ to account for quantized vibrations orthogonal to ξ, the reaction coordinate along which the PMF is defined, at the maximum of the PMF, $\xi*$; $\Delta W_{vib,R}(T)\Delta W_{vib,R}(T)$ corrects $W^{CM}(T,\xi_R)$ $W^{CM}(T,z_R)$ for quantized vibrations at the reactant side minimum of the PMF, ξ_R, and $G_{R,T,F}^{CM}$ $G_{R,T,F}^{CM}$ is a correction for the vibrational free energy of the reactant mode that correlates with motion along the reaction coordinate.[4]

Grote-Hynes theory allow one to obtain the recrossing transmission coefficient through the ratio between the reactive frequency, ω_r, and the equilibrium barrier frequency, ω_{eq}, as shown in equation (2):[5]

$$\gamma_{GH}=\frac{\omega_r}{\omega_{eq}} \quad (2)$$

The equilibrium frequency was obtained from PMFs for the reaction in the enzyme, using a parabolic fit around the TS region:. The same procedure than before was carried out to obtain the PMFs, but using a small range of the reaction coordinate values around TS region (approximately 0.15 Å), and fitted them to a parabolic function:

$$\Delta PMF=-\frac{1}{2}k_{eq}\left(\xi-\xi^{\ddagger}\right)^2 \quad (3)$$

where ΔPMF is the potential of mean force difference with respect to the maximum in the profile, k_{eq} is the equilibrium force constant and $\xi^{\ddagger}$ is the reaction coordinate of the maximum of the profile. Consequently, the equilibrium frequency is

$$\omega_{eq}=\frac{1}{2\pi c}\sqrt{\frac{k_{eq}}{\mu_{\xi}}} \quad (4)$$

where μ_{ξ} is the reaction coordinate reduced mass and c is the speed of light.

Once the equilibrium frequency is known, the reactive frequency can be obtained via the GH equation:[6,7]

$$\omega_r^2 - \omega_{eq}^2 + \omega_r \int_0^\infty \zeta_{TS}(t) e^{-\omega_r t} dt = 0 \qquad (5)$$

The friction kernel ($\zeta_{TS}(t)$) can be obtained from the autocorrelation of the forces projected on the reaction coordinate obtained from simulation where the system is kept at the TS:[5]

$$\zeta_{TS}(t) = \frac{\left\langle F_\xi(0) F_\xi(t) \right\rangle_{\xi=\xi^*}}{\mu_\xi k_B T} \qquad (6)$$

where k_B is the Boltzmann constant, T is the temperature and $\zeta_{TS}(t)$ quantifies the dynamical coupling of the protein motion to the reaction coordinate ξ. The equilibrium frequency, ω_{eq}, does not depend on the mass, so it is the same for the four isotopologues. However, the reactive frequency, ω_r, does depend on the mass of each isotopologue through the friction kernel, $\zeta_{TS}(t)$.

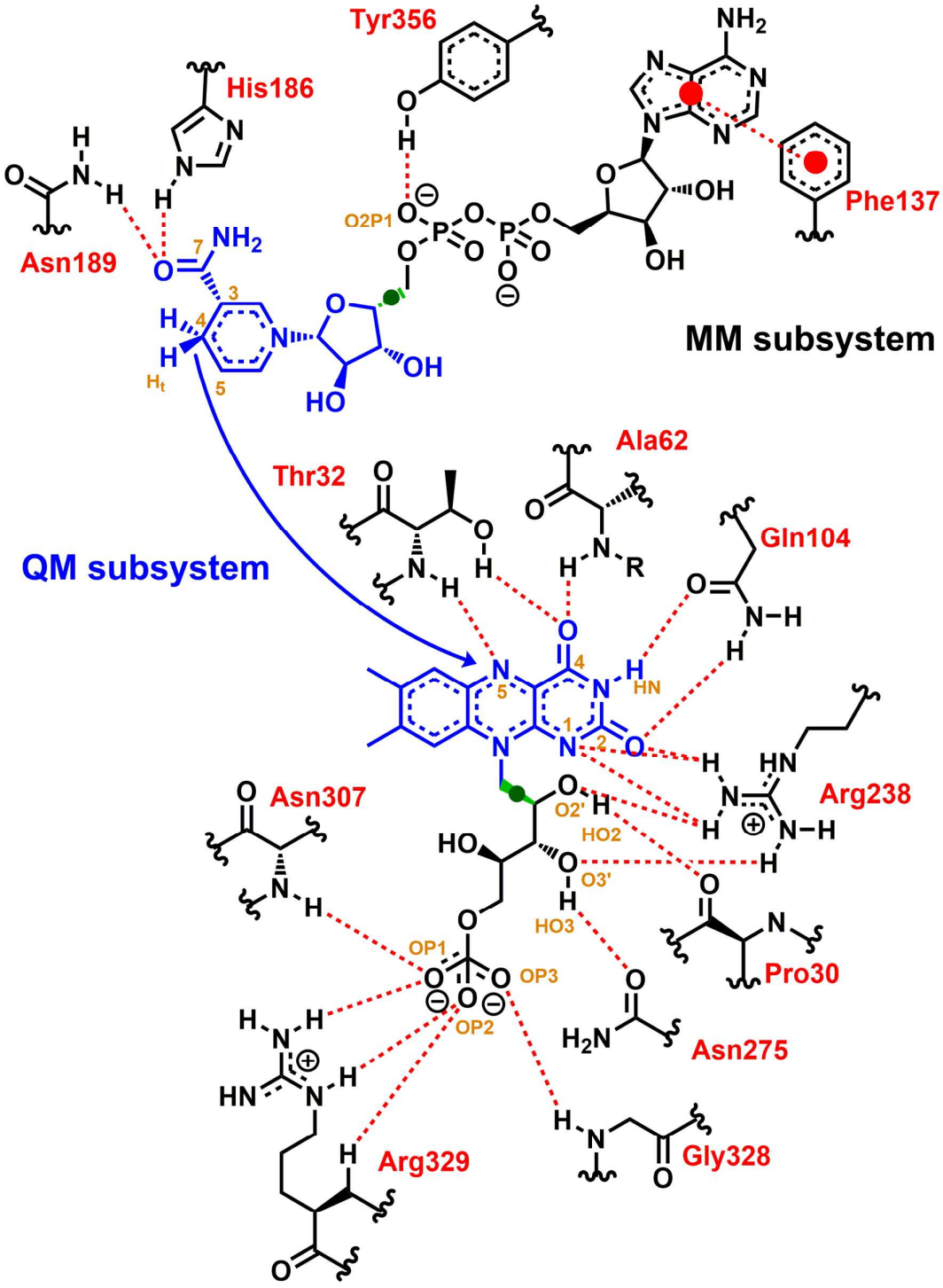

Scheme S1. Representation of the active site of MR showing the QM/MM partitioning scheme. QM part is colored in blue while MM part is colored in black. Green circles represent the quantum hydrogen link atoms. Key amino acids are included to describe the most important interactions between substrate/cofactor and enzyme. Interacting atoms in substrate/cofactor have been labeled in orange.

Table S5. Energy barriers and stationary points key distances for hydride transfer reaction in MR enzyme by using AM1, RM1 and B3LYP-D3/6-31G(d,p).

		AM1	RM1	B3LYP-D3	RM1 with spline correctionss
$\Delta E^{\ddagger}$		40.2	13.3	14.1	14.1
$\Delta E_{reaction}$		14.6	6.2	5.5	6.1
RS	**$\alpha(C4_{cofac}\text{-}H_t\text{-}N5_{subs})$**	130.2	151.9	133.4	137.7
	$d(C4_{cofac}\text{-}H_t) - d(N5_{subs}\text{-}H_t)$	-2.11	-1.08	-1.59	-1.41
	$d(C4_{cofac}\text{-}N5_{subs})$	4.03	3.21	3.55	3.42
	$d(C4_{cofac}\text{-}H_t)$	1.11	1.11	1.10	1.11
	$d(N5_{subs}\text{-}H_t)$	3.22	2.19	2.69	2.52
TS	**$\alpha(C4_{cofac}\text{-}H_t\text{-}N5_{subs})$**	172.0	163.0	160.4	162.9
	$d(C4_{cofac}\text{-}H_t) - d(N5_{subs}\text{-}H_t)$	0.17	0.09	0.09	0.09
	$d(C4_{cofac}\text{-}N5_{subs})$	2.74	2.64	2.65	2.64
	$d(C4_{cofac}\text{-}H_t)$	1.46	1.38	1.39	1.38
	$d(N5_{subs}\text{-}H_t)$	1.29	1.29	1.30	1.29
PS	**$\alpha(C4_{cofac}\text{-}H_t\text{-}N5_{subs})$**	164.7	155.4	139.0	145.5
	$d(C4_{cofac}\text{-}H_t) - d(N5_{subs}\text{-}H_t)$	1.78	1.35	1.07	1.01
	$d(C4_{cofac}\text{-}N5_{subs})$	3.81	3.35	2.96	2.95
	$d(C4_{cofac}\text{-}H_t)$	2.81	2.39	2.10	2.04
	$d(N5_{subs}\text{-}H_t)$	1.03	1.03	1.03	1.03

Table S6. Key averaged structural parameters of RS from 100 ns MM simulation by using a CHARMM General Force Field with the NAMD program, performed at 298 K. Distances are in Å and angles in degrees.

	RS
$\alpha(C4_{cofac}\text{-}H_t\text{-}N5_{subs})$	144 ± 20
$d(C4_{cofac}\text{-}H_t) - d(N5_{subs}\text{-}H_t)$	-1.69 ± 0.4
$d(C4_{cofac}\text{-}N5_{subs})$	3.6 ± 0.4
$d(C4_{cofac}\text{-}H_t)$	1.11
$d(N5_{subs}\text{-}H_t)$	2.7 ± 0.5

Table S7. Key averaged structural parameters of RS, TS and PS from 100 ps MD simulation at AM1/MM level performed at 298 K. Distances are in Å and angles in degrees.

	RS	**TS**	**PS**
$\alpha(C4_{cofac}\text{-}H_t\text{-}N5_{subs})$	147 ± 12	161 ± 8	162 ± 8
$d(C4_{cofac}\text{-}H_t) - d(N5_{subs}\text{-}H_t)$	-1.56 ± 0.04	0.06 ± 0.04	0.96 ± 0.03
$d(C4_{cofac}\text{- }N5_{subs})$	3.65 ± 0.10	2.45 ± 0.07	2.97 ± 0.07
$d(C4_{cofac}\text{-}H_t)$	1.11 ± 0.04	1.27 ± 0.04	1.98 ± 0.04
$d(N5_{subs}\text{-}H_t)$	2.67 ± 0.05	1.22 ± 0.04	1.03 ± 0.03
$d(O7N_{cofac}\text{-}HE2_{HIS186})$	1.88 ± 0.13	1.87 ± 0.12	1.89 ± 0.12
$d(O7N_{cofac}\text{-}HD21_{ASN189})$	2.03 ± 0.21	2.2 ± 0.3	2.3 ± 0.3
$d(O7N_{cofac}\text{-}ND2_{ASN189})$	3.00 ± 0.19	3.11 ± 0.24	3.18 ± 0.24
$d(O2P1_{cofac}\text{-}HH_{TYR356})$	1.8 ± 0.4	1.56 ± 0.10	1.57 ± 0.10
$d(Ø_{adenine,\ subs}\text{-}Ø_{Phe137})$	4.2 ± 0.3	4.2 ± 0.3	3.95 ± 0.18
$d(N5_{subs}\text{-}H_{THR132})$	1.92 ± 0.10	2.04 ± 0.11	1.99 ± 0.11
$d(O4_{subs}\text{-}HG1_{THR132})$	1.99 ± 0.15	1.92 ± 0.12	1.89 ± 0.12
$d(O4_{subs}\text{-}H_{ALA62})$	2.7 ± 0.3	2.7 ± 0.3	2.7 ± 0.3
$d(HN_{subs}\text{-}OE1_{GLN104})$	1.96 ± 0.16	1.97 ± 0.15	2.01 ± 0.16
$d(O2_{subs}\text{-}HE22_{GLN104})$	2.11 ± 0.19	2.07 ± 0.17	2.04 ± 0.16
$d(O2_{subs}\text{-}HH11_{ARG238})$	2.01 ± 0.14	1.98 ± 0.13	1.93 ± 0.12
$d(N1_{subs}\text{-}HH11_{ARG238})$	2.52 ± 0.14	2.50 ± 0.14	2.50 ± 0.14
$d(N1_{subs}\text{-}HH12_{ARG238})$	2.64 ± 0.17	2.58 ± 0.17	2.57 ± 0.16
$d(N1_{subs}\text{-}NH1_{ARG238})$	2.98 ± 0.10	2.96 ± 0.10	2.95 ± 0.10
$d(O2'_{subs}\text{-}HH12_{ARG238})$	1.94 ± 0.18	1.93 ± 0.18	1.90 ± 0.16
$d(HO2_{subs}\text{-}O_{PRO30})$	2.04 ± 0.19	1.97 ± 0.17	1.93 ± 0.16
$d(O3'_{subs}\text{-}HH22_{ARG238})$	2.03 ± 0.21	2.01 ± 0.21	1.96 ± 0.20
$d(HO3_{subs}\text{-}OD1_{ASN275})$	2.3 ± 0.3	2.3 ± 0.3	2.2 ± 0.3
$d(OP1_{subs}\text{-}H_{ASN307})$	2.1 ± 0.3	2.1 ± 0.3	1.85 ± 0.22
$d(OP1_{subs}\text{-}HH11_{ARG329})$	1.58 ± 0.17	2.1 ± 0.3	1.53 ± 0.10
$d(OP2_{subs}\text{-}HE_{ARG329})$	2.2 ± 0.4	2.1 ± 0.3	1.93 ± 0.24
$d(OP2_{subs}\text{-}H_{ARG329})$	1.79 ± 0.13	1.72 ± 0.12	1.77 ± 0.12
$d(OP3_{subs}\text{-}H_{GLY328})$	1.74 ± 0.14	1.74 ± 0.14	1.74 ± 0.15

Table S8. QMT coefficient, κ, at 298 K for every snapshot structure.

Snapshot	HH	DH	HD	DD
1	18.1350	11.7440	13.3200	9.8500
2	26.4160	12.1810	19.3020	10.7400
3	18.8090	9.9343	14.3290	8.7351
4	16.0500	9.0398	12.9440	7.8695
5	20.0141	9.7592	14.6750	8.2463
6	21.7150	10.1760	15.8890	8.7924
7	32.8020	15.4500	24.2180	13.6190
8	23.0410	11.5080	16.2690	9.6194
9	29.0580	14.4100	22.1390	12.7580
10	28.3550	11.8610	17.2380	10.3050
11	27.9800	13.3530	20.2910	11.6810
12	17.1320	6.3664	11.5730	5.5118
13	33.2540	14.8340	20.9150	12.8260
14	18.1430	9.7750	12.9180	9.2246
15	14.1010	8.8542	11.1580	8.1715
16	26.4080	12.5010	20.4400	10.8790
17	19.6950	9.6858	14.7560	8.4372
18	31.9950	14.3880	24.3110	12.8380
19	25.1440	9.8700	19.2410	8.4852
20	28.6870	12.6360	21.1340	10.9700
21	21.2150	11.1260	15.6960	9.7034
22	22.2830	10.4410	16.6830	9.0644
23	19.1670	9.5640	14.6300	8.3580
24	27.8750	12.9630	21.1230	11.4950
25	26.3200	12.0930	20.5300	10.5030
AVERAGE	**23.7518**	**11.3805**	**17.4289**	**9.9473**
SD	**5.4766**	**2.1662**	**3.8691**	**1.9112**

Table S9. Average and standard deviation of QMT coefficient, κ, for HH and DH isotopologues at 278, 298 and 313K.

	278		
	HH	DH	K_D/κ_H
AVERAGE	38.4731	19.5234	2.0570
SD	7.0835	3.3461	0.3954

	298		
	HH	DH	K_D/κ_H
AVERAGE	23.7518	11.3805	2.0854
SD	5.4766	2.1662	0.2544

	313		
	HH	DH	K_D/κ_H
AVERAGE	16.359	8.4226	1.9547
SD	7.2448	3.4667	0.3543

Additional References

(1) Hay, S.; Pudney, C. R.; Hothi, P.; Scrutton, N. S. *J Phys Chem A* **2008**, *112*, 13109.

(2) Hobbs, J. K.; Jiao, W.; Easter, A. D.; Parker, E. J.; Schipper, L. A.; Arcus, V. L. *ACS chemical biology* **2013**, *8*, 2388.

(3) Arcus, V. L.; Prentice, E. J.; Hobbs, J. K.; Mulholland, A. J.; Van der Kamp, M. W.; Pudney, C. R.; Parker, E. J.; Schipper, L. A. *Biochemistry* **2016**, *55*, 1681.

(4) Alhambra, C.; Corchado, J.; Sánchez, M. L.; Garcia-Viloca, M.; Gao, J.; Truhlar, D. G. *J. Phys. Chem. B* **2001**, *105*, 11326.

(5) Gertner, B. J.; Wilson, K. R.; Hynes, J. T. *J. Chem. Phys.* **1989**, *90*, 3537.

(6) Grote, R. F.; Hynes, J. T. *J. Chem. Phys.* **1980**, *73*, 2715.

(7) Hynes, J. T. *The Theory of Chemical Reactions Dynamics*; Baer, M.: CRC Press, Boca Raton, FL, 1985.